Published in final edited form as:
Biochemistry. 2007 January 16; 46(2): 534–542. doi:10.1021/bi061859h.

Oxyferryl Heme and Not Tyrosyl Radical Is the Likely Culprit in Prostaglandin H Synthase-1 Peroxidase Inactivation†

Gang Wu[‡,§], **Corina E. Rogge**[‡], **Jinn-Shyan Wang**[‖], **Richard J. Kulmacz**[‡], **Graham Palmer**[⊥], and **Ah-Lim Tsai**[‡,*]

[‡]Department of Internal Medicine, University of Texas Health Science Center, Houston, Texas 77030

[‖]School of Medicine, Fu Jen Catholic University, Taipei Hisen, Taiwan 24205

[⊥]Department of Biochemistry and Cell Biology, Rice University, Houston, Texas 77005

Abstract

Prostaglandin H synthase-1 (PGHS-1) is a bifunctional heme protein catalyzing both a peroxidase reaction, in which peroxides are converted to alcohols, and a cyclooxygenase reaction, in which arachidonic acid is converted into prostaglandin G_2. Reaction of PGHS-1 with peroxide forms Intermediate I, which has an oxyferryl heme and a porphyrin radical. An intramolecular electron transfer from Tyr385 to Intermediate I forms Intermediate II, which contains two oxidants: an oxyferryl heme and the Tyr385 radical required for cyclooxygenase catalysis. Self-inactivation of the peroxidase begins with Intermediate II, but it has been unclear which of the two oxidants is involved. The kinetics of tyrosyl radical, oxyferryl heme, and peroxidase inactivation were examined in reactions of PGHS-1 reconstituted with heme or mangano protoporphyrin IX with a lipid hydroperoxide, 15-hydroperoxyeicosatetraenoic acid (15-HPETE), and ethyl hydrogen peroxide (EtOOH). Tyrosyl radical formation was significantly faster with 15-HPETE than with EtOOH and roughly paralleled oxyferryl heme formation at low peroxide levels. However, the oxyferryl heme intensity decayed much more rapidly than the tyrosyl radical intensity at high peroxide levels. The rates of reactions for PGHS-1 reconstituted with MnPPIX were approximately an order of magnitude slower, and the initial species formed displayed a wide singlet (WS) radical, rather than the wide doublet radical observed with PGHS-1 reconstituted with heme. Inactivation of the peroxidase activity during the reaction of PGHS-1 with EtOOH or 15-HPETE correlated with oxyferryl heme decay, but not with changes in tyrosyl radical intensity or EPR line shape, indicating that the oxyferryl heme, and not the tyrosyl radical, is responsible for the self-destructive peroxidase side reactions. Computer modeling to a minimal mechanism was consistent with oxyferryl heme being the source of peroxidase inactivation.

Prostagladin H synthases (PGHSs) catalyze the first two steps in biosynthesis of prostaglandins, the cyclooxygenase reaction that converts arachidonic acid (AA)[1] to prostaglandin (PG)G_2 and the peroxidase reaction that reduces PGG_2 to PGH_2 (1). The cyclooxygenase reaction is dependent upon formation of the Tyr385 radical during the peroxidase reaction (2). A simplified mechanistic model is shown in Figure 1. According to

†This work was supported by U.S. Public Health Service Grants GM44911 (to A.-L.T.), GM52170 (to R.J.K.), and GM55807 (to G.P.) and Postdoctoral Fellowship DK61929 (to C.E.R.), and Welch Foundation Grant C636 (to G.P.).

*To whom correspondence should be addressed: Division of Hematology, University of Texas Health Science Center, P.O. Box 20708, Houston, TX 77225. Telephone: (713) 500-6771. Fax: (713) 500-6810. Ah-Lim.Tsai@uth.tmc.edu.
§Current address: Department of Biochemistry and Cell Biology, Rice University, Houston, TX 77005.

this model, resting PGHS first reacts with peroxide and generates Intermediate I, an oxidized species that contains oxyferryl heme and a porphyrin cation radical in the peroxidase active site. An intramolecular electron transfer converts Intermediate I to Intermediate II, which contains two oxidants: oxyferryl heme, or Compound II, in the peroxidase site and a tyrosyl radical on residue 385 in the cyclooxygenase channel (3–5). The Tyr385 radical abstracts the *pro-S* hydrogen atom from C13 of AA, initiating cyclooxygenase catalysis and PGG_2 formation (6).

Reaction with peroxide drives the redox events that lead to strong feedback amplification of cyclooxygenase catalysis, and it also drives the irreversible self-inactivation of both peroxidase and cyclooxygenase activities that imposes an upper limit on prostanoid synthesis (7,8). Cyclooxygenase inactivation induced by peroxide occurs on the same time scale as peroxidase inactivation, although the former seems more sensitive to the peroxide structure (9,10). Intermediate II is the starting point for peroxide-induced peroxidase inactivation (9). However, it remains unclear which of the two oxidants generated after reaction with peroxide, the oxyferryl heme or the tyrosyl radical, is the damaging species.

Earlier analyses of PGHS-1 peroxidase kinetics relied primarily on rapid-scan stopped-flow measurements (3,4,11). Tyrosyl radical kinetic studies using rapid-freeze quench and EPR methods were conducted primarily with convenient, water soluble peroxides such as EtOOH (12), and more physiologically relevant lipid peroxides have not been investigated in detail. The kinetic relationship between the oxyferryl heme and the tyrosyl radical present in Intermediate II has not been thoroughly tested by parallel stopped-flow and RFQ EPR kinetic measurements in PGHS-1, although there are indications that kinetic divergence of oxyferryl heme and tyrosyl radical can occur in PGHS-2 (12). In this study, the kinetics of oxyferryl heme and tyrosyl radical formation and decay and of peroxidase inactivation were examined in reactions of PGHS-1 with a lipid peroxide, 15-(*S*)-HPETE, at different heme to peroxide ratios. This long-chain fatty acid peroxide is a cyclooxygenase side product (13) and is much closer in physical characteristics and peroxidase kinetic parameters to PGG_2 than is EtOOH (11,14). To improve the discriminating power, the kinetic analyses were conducted with native PGHS-1, with Mn-PGHS-1, which has impaired peroxidase catalysis (15–17), and with native PGHS-1 complexed with indomethacin, which selectively impairs cyclooxygenase catalysis (18). Correlated kinetic data for both the heme group and the tyrosyl radical in this study strongly support their independent decay kinetics and suggest that it is the oxyferryl heme, and not the tyrosyl radical, that is the dominant oxidant in peroxidase inactivation. This conclusion is consistent with computer fitting to a minimal model for PGHS peroxidase catalysis and self-inactivation.

EXPERIMENTAL PROCEDURES

Materials

Heme was purchased from Sigma (St. Louis, MO) or Porphyrin Products, Inc. (Logan, UT). MnPPIX was obtained from Porphyrin Products, Inc. EtOOH was purchased as a 5% aqueous solution from Polysciences Inc. (Warrington, PA) or obtained as a 6.25% solution from G. Barney Ellison (University of Colorado, Boulder, CO). 15-HPETE was prepared from AA using soybean lipoxygenase (19). The purity of 15-HPETE was assessed using HPLC, and its concentration was determined by measuring the oxidation of TMPD catalyzed by excess Fe-

[1]Abbreviations: AA, arachidonic acid; PGHS-1, prostaglandin H synthase-1; PGHS-2, prostaglandin H synthase-2; Fe-PGHS-1, PGHS-1 reconstituted with hemin; MnPPIX, magano protoporphyrin IX; Mn-PGHS-1, PGHS-1 reconstituted with MnPPIX; indo-PGHS-1, indomethacin-treated Fe-PGHS-1; 15-HPETE, 15-hydroperoxyeicosatetraenoic acid; EtOOH, ethyl hydrogen peroxide; EPR, electron paramagnetic resonance; TMPD, *N*,*N*,*N*′,*N*′-tetramethyl-*p*-phenylenediamine; WD, wide doublet EPR signal; NS, narrow singlet EPR signal; WS, wide singlet EPR signal; RFQ, rapid freeze-quench.

PGHS-1. Tween 20 was purchased from Pierce (Rockford, IL) or Anatrace (Maumee, OH). All other reagents were obtained from Sigma-Aldrich.

PGHS-1 was prepared in its apoenzyme form from ram seminal vesicles (20), with 5 mM glutathione included in the isoelectric focusing step. Fe-PGHS-1 and Mn-PGHS-1 were prepared by incubating the apoenzyme with heme or mangano protoporphyrin IX (17). Indomethacin-treated Fe-PGHS-1 was prepared by incubating a 1.5-fold molar excess of indomethacin with Fe-PGHS-1 at room temperature until the cyclooxygenase activity fell below 4% of the initial value. The amount of endogenous cosubstrate present in the purified Fe-PGHS-1 was determined by EtOOH titration at several different concentrations of hydroquinone (21). Briefly, the amount of EtOOH necessary to completely oxidize Fe-PGHS-1 in the presence of different levels of hydroquinone was obtained by monitoring ΔA_{410} (bleaching of ferric heme Soret peak). A secondary plot of the EtOOH equivalents required for maximal ΔA_{410} as a function of the hydroquinone concentration was linear, with the *y*-intercept giving an estimate of endogenous cosubstrate (in terms of hydroquinone). A value of 8–9 equiv of endogenous cosubstrate was determined for the PGHS-1 preparations used in this study.

Stopped-Flow Kinetics

Optical stopped-flow kinetic measurements were conducted using a Bio-Sequential DX-18MV stopped-flow instrument (Applied Photophysics, Leatherhead, U.K.). The kinetics of formation of Intermediate II or Compound II (oxyferryl heme) in Fe-PGHS-1 were followed using the absorbance increases at 428, 524, or 560 nm. Formation of Mn(IV)=O in Mn-PGHS-1 was monitored by absorbance increases at 400 or 420 nm. Apparent rate constants, k_{obs}, for both formation and decay phases of oxyferryl heme and Mn(IV)=O, were obtained by fitting kinetic traces to a single-exponential function.

Peroxidase Inactivation

Sequential, two-stage mixing was used for measurement of peroxidase inactivation kinetics as previously published (9). Briefly, in the first stage of mixing, PGHS-1 was reacted with peroxide for different periods of time. In the second stage, the reaction mixture from the first stage was mixed with 10 mM guaiacol and 10 mM H_2O_2 and surviving peroxidase activity was followed optically by the increase in A_{436} due to guaiacol oxidation. The apparent rate constant for peroxidase inactivation, k_{obs}, was obtained by fitting the decrease in surviving peroxidase activity as a function of the first-stage incubation time to a single-exponential equation.

Rapid-Freeze Quench EPR

RFQ experiments used a System 1000 chemical/freeze quench apparatus with a model 1019 syringe ram, a model 715 ram controller, and a 0.008 in. nozzle (Update Instrument, Inc., Madison, WI). The ram velocity was 2.0 cm/s, and the dead time of the instrument was 4–5 ms. An isopentane bath at 125–130 K was used to chill the packing assembly for sample collection and pressure filtration packing (22).

EPR Spectroscopy

EPR spectra of samples were recorded with either a Varian E-6 or a Bruker EMX EPR spectrometer. Radical concentrations were determined by double integration of the EPR signals with reference to a copper standard (23), with a correction factor of 0.45 for packing (22).

Global Analysis of EPR Data

Global analysis of the RFQ-EPR data was conducted using the Pro-K software package from Applied Photophysics, which utilizes a Marquardt–Levenberg algorithm for least-squares analysis. The data were fit to a simple four-state model with three rate constants (eq 1).

$$\underset{\text{PGHS-1}}{\text{EPR silent}}+\text{peroxide} \xrightarrow{k_1} \text{WD} \xrightarrow{k_2} \text{NS} \xrightarrow{k_3} \underset{\text{PGHS-1}}{\text{EPR silent}} \quad (1)$$

The k_1 step represents the bimolecular reaction of PGHS-1 with peroxide; given the high peroxide concentration that was used, the fast reaction rate, and the low K_M for peroxide, this step was treated as a pseudo-first-order reaction.

Computer Simulation of the Kinetics of Soret Absorbance Changes and Peroxidase Inactivation

Mathematical simulation was conducted using SCoP version 3.52 (Simulation Resources, Inc., Redlands, CA) with a PRAXIS fitting algorithm. The kinetic model block included a minimal number of steps for the peroxidase catalytic cycle and its self-inactivation (Figure 1); the equations and rate constants used in the least-squares fitting to the mathematic model are listed in Table 1. E, E_I, E_II, E_III, and E_in correspond to resting ferric PGHS-1, Intermediate I, Compound II, the self-inactivated intermediate, and the terminal inactivated PGHS-1, respectively. Conversion of E_I to E_II (step b). was considered to form two discrete species: Compound II (oxyferryl heme), which can undergo further peroxidase reactions, and tyrosyl radical. ROOH is the peroxide and ROH the corresponding alcohol. Red and Red_o are the endogenous reductant (cosubstrate) and its reacted (oxidized) form, respectively; 8.5 equiv of endogenous cosubstrate per protein monomer was used, based on hydroquinone/peroxide titration measurements. Irreversible reactions were assumed for each step. Step d allows the one-electron recycling of oxyferryl back to ferric heme without affecting the tyrosyl radical. In other words, once Intermediate II (Compound II with tyrosyl radical) is formed, the tyrosyl radical ($Tyr^{\bullet}$) concentration is uncoupled from the redox cycling of the heme component.

Equations g–k are the mass balance equations and the expressions for the surviving peroxidase activity, and A_{428}, absorbance at 428 nm, is contributed mainly by Coupound II (E_II). PeroxideTotal is the initial concentration of peroxide. Constants ε1–ε4 are molar absorbance coefficients for individual enzyme intermediates (11,24). The remaining peroxidase activity contributed by Intermediate III and the terminal inactivated complex after treatment with peroxide is represented as Residual in eq j.

The floating parameters being fitted are k_1–k_6, Residual, and ε1–ε4, with k_1, k_2, and ε1– ε4 constrained within 20% of the published values (11). k_3 and k_4 were limited between 10^4 and 10^5 M^{-1} s^{-1}. k_5 values were constrained between 0.1 and 1 s^{-1}, and $_{k6}$ values were limited between 0.001 and 0.1 s^{-1}. Residual was varied between 0 and 0.4. Predictions for both the absorbance change at 428 nm, A_{428}, and the normalized peroxidase activity, Active, were generated simultaneously using the same set of parameter values.

RESULTS

Kinetics of Tyrosyl Radical and Oxyferryl Heme Formation and Decay in Fe-PGHS-1 at Low 15-HPETE Ratios

Reaction of 15 μM Fe-PGHS-1 with either 2 or 5 equiv of 15-HPETE resulted in the rapid formation of tyrosyl radical detected by RFQ-EPR (Figure 2 and Figure 3). An initial 34 G wide doublet EPR signal (WD) was formed at similar rates under both reaction conditions, 33

± 5 s^{-1} for the reaction with 5 equiv of 15-HPETE and 59 ± 17 s^{-1} during the reaction with 2 equiv of 15-HPETE, with essentially first-order behavior despite second-order conditions. During the reaction with 5 equiv of 15-HPETE, the tyrosyl radical intensity plateaued after 0.2 s and later began a slow monoexponential decay (0.16 ± 0.03 s^{-1}) that was accompanied by conversion from the WD spectrum to a wide singlet (WS) (data not shown). The tyrosyl radical had roughly similar decay kinetics (0.06 ± 0.02 s^{-1}) at the lower 15-HPETE concentration.

Formation of oxyferryl heme in the reaction of Fe-PGHS-1 with peroxide under the reaction conditions used in the RFQ experiments described above was characterized by a shift of the Soret absorbance from 410 to 428 nm and by an increase in the intensity of the α and β bands at 560 and 524 nm. With 5 equiv of 15-HPETE, the oxyferryl heme species was formed at a rate of 112 ± 1 s^{-1}, measured at 428 nm; the rates obtained at 524 and 560 nm were 123 ± 8 and 115 ± 13 s^{-1}, respectively. The reaction proceeded at a similar rate (monitored by A_{428}) when 2 equiv of 15-HPETE was used (90 ± 1 s^{-1}). Because the Fe-PGHS-1 and peroxide concentrations that were used were quite high, formation of Intermediate I was complete within the dead time of the instrument, and the observed rates reflect formation of Intermediate II oxyferryl heme. At both concentrations of 15-HPETE, formation of oxyferryl heme reached a maximum at 70–80 ms and decayed after ~100 ms. Decay of oxyferryl heme was a multistep process with an overall rate of 0.016 ± 0.002 s^{-1} when 5 equiv of 15-HPETE was used (Figure 3A). Decay of the tyrosyl radical intensity (1.0 ± 0.7 s^{-1}) was slower than that of oxyferryl heme (2.9 ± 0.01 s^{-1}) when 2 equiv of 15-HPETE was used (Figure 3B).

Kinetics of Tyrosyl Radical and Mn(IV)=O in Mn-PGHS-1

Reaction of Mn-PGHS-1 with 2 or 5 equiv of 15-HPETE resulted in formation of a 35 G WS spectrum (Figure 4), without prior formation of a WD species analogous to that observed with Fe-PGHS-1 (Figure 2). The WS tyrosyl radical in Mn-PGHS-1 formed at rates of 1.8 ± 0.2 and 3 ± 1 s^{-1} with 2 and 5 equiv of 15-HPETE, respectively (Figure 5). The tyrosyl radical signal decayed at 0.1 ± 0.3 s^{-1} during the reaction with 2 equiv of 15-HPETE and at 0.3 ± 0.3 s^{-1} during the reaction with 5 equiv of the peroxide.

Formation of Mn^{4+}=O, equivalent to oxyferryl heme in Fe-PGHS-1, was followed by the absorbance increase at 420 nm (Figure 5). The rate of formation was 7.9 ± 0.1 s^{-1} when 19 μM Mn-PGHS-1 was reacted with 5 equiv of 15-HPETE (Figure 5A) and 4.9 ± 0.0 s^{-1} when 20 μM Mn-PGHS-1 was reacted with 2 equiv of 15-HPETE (Figure 5B). Mn^{4+}=O decayed slowly in a multistep process with overall rates of 0.17 ± 0.00 and 0.13 ± 0.00 s^{-1} for the reactions with 5 and 2 equiv of 15-HPETE, respectively. Similar rate constants were obtained from absorbance changes at 400 nm (data not shown).

Kinetics of Peroxidase Activity, Tyrosyl Radical, and Oxyferryl Heme of Fe-PGHS-1 during Reaction with 20 equiv of EtOOH

The kinetics of tyrosyl radical and oxyferryl heme decay could not both be determined under the reaction conditions used in our earlier study (9). To directly compare the kinetics of peroxidase inactivation with those of oxyferryl heme and tyrosyl radical formation and decay, the study presented here utilizes a higher enzyme concentration (30 μM) and a higher peroxide/enzyme ratio (20). These reaction conditions resulted in peroxidase inactivation at a rate of 0.18 ± 0.03 s^{-1} (Figure 6A), with ~30% activity remaining at the longest incubation times. This decay in peroxidase activity contrasts with the kinetics observed for tyrosyl radical intensity under the same conditions. The radical formed quickly (12 ± 7 s^{-1}) and reached a stable maximum of ~0.5 spin/heme. Between 500 ms and 30 s, the tyrosyl radical EPR signal line shape converted from a WD to a WS (Figure 6B), the latter being the sum of the WD and the narrow singlet (NS) ascribed to the self-inactivated enzyme (25,26). To compare the kinetics of this conversion with those of peroxidase inactivation, the WD and NS were resolved

by global analysis. This analysis indicated that the WD → NS conversion occurred at 0.19 ± 0.3 s^{-1}. Under the same conditions, oxyferryl heme formed at a rate of 63 ± 1 s^{-1} (from A_{428} changes), while decay of oxyferryl heme appeared to occur in multiple steps, with an overall rate of 0.14 ± 0.01 s^{-1}.

Kinetics of Peroxidase Activity, Tyrosyl Radical, and Oxyferryl Heme during the Reaction of Fe-PGHS-1 with 20 equiv of 15-HPETE

Compared to the reaction with EtOOH just described, the peroxidase activity was lost more quickly (1.1 ± 0.1 s^{-1}) when 30 μM Fe-PGHS-1 was reacted with 20 equiv of 15-HPETE (Figure 7, top panel). Furthermore, less than 4% of the initial peroxidase activity survived after extended reaction times. The tyrosyl radical formed within the dead time of the instrument, plateaued for 2 s, and then slowly decayed at a rate of 0.004 ± 0.001 s^{-1}. The rate constant for the WD → NS conversion was 0.25 ± 0.04 s^{-1} (Figure 7, bottom panel). Under the same conditions, oxyferryl heme formed during the dead time of the instrument and reached its maximum by 10 ms. Decay of oxyferryl heme appeared to be biphasic, with rate constants of 0.94 ± 0.01 and 0.11 ± 0.01 s^{-1}, corresponding to 45 and 55%, respectively, of the overall absorbance change. Thus, the kinetics of peroxidase inactivation paralleled those of the fast phase of oxyferryl heme decay, and both were faster than the kinetics of the WD → NS conversion or the tyrosyl radical decay.

Kinetics of Peroxidase Activity, Tyrosyl Radical, and Oxyferryl Heme during the Reaction of Indomethacin-Treated Fe-PGHS-1 with 20 equiv of 15-HPETE

Pretreatment with indomethacin inhibits cyclooxygenase activity and affects the EPR signal produced by reaction with peroxides, with a 29 G NS species formed irrespective of reaction time (12). Pretreatment with indomethacin had little effect on peroxidase inactivation by 15-HPETE, which occurred with a rate of 1.1 ± 0.1 s^{-1} (Figure 8A), the same as that for untreated Fe-PGHS-1 under the same conditions (Figure 7). Residual peroxidase activity at 50 s was less than 4% of starting activity, the same as that with uninhibited Fe-PGHS-1 (Figure 7). The RFQ-EPR results for the reaction of indomethacin-treated Fe-PGHS-1 with 20 equiv of 15-HPETE (Figure 8B) showed that a weak NS signal formed within the dead time of the instrument and approximately doubled in intensity over the next 5 s to reach a plateau of approximately 0.1 spin/heme. This maximum concentration of tyrosyl radical was less than one-third of that obtained with Fe-PGHS-1 itself (Figure 7). As seen with Fe-PGHS-1, formation of oxyferryl heme in indomethacin-treated Fe-PGHS-1 was fast and reached its maximum by 10 ms. The subsequent decay of oxyferryl heme in indomethacin-treated Fe-PGHS-1 also appeared to be biphasic, with rates of 0.81 ± 0.01 and 0.084 ± 0.001 s^{-1}, corresponding to 43 and 56%, respectively, of the observed absorbance changes (Figure 8, top panel). Thus, peroxidase inactivation kinetics in indomethacin-treated Fe-PGHS-1 paralleled those of the decay of oxyferryl heme and not those of tyrosyl radical decay.

DISCUSSION

Formation and Decay of Tyr385 Radical and Oxyferryl Heme during Reaction of 15-HPETE with Fe-PGHS-1

15-HPETE is useful as a PGHS peroxidase substrate because it is structurally similar to the natural substrate, PGG_2, yet much less prone to decomposition in aqueous solution. As in the reactions with EtOOH, a WD EPR signal formed when Fe-PGHS-1 was reacted with 15-HPETE, but at a 2-fold greater rate (33 s^{-1} vs 16 s^{-1}) (12). This was consistent with a previous study showing 15-HPETE to be a more efficient peroxide than EtOOH (11). The rate of oxyferryl heme formation was also faster in the reaction with 15-HPETE than with EtOOH. Interestingly, the rate of oxyferryl heme formation (112 s^{-1}) was significantly faster than the rate of tyrosyl radical formation (33 s^{-1}). A similar difference was observed in reactions with

EtOOH (12) and may be due to the inherent noise in RFQ measurements (e.g., Figure 3). The general correspondence between rates of oxyferryl heme and tyrosyl radical formation with the water-soluble peroxide, EtOOH, and the lipid peroxide, 15-HPETE, is consistent with the peroxidase portion of the PGHS mechanism in Figure 1.

Independent Decay of Oxyferryl Heme and Tyrosyl Radical

The relationship between tyrosyl radical and oxyferryl heme decay was dependent on the peroxide level. In reactions with 5 equiv of EtOOH or 15-HPETE, the tyrosyl radical intensity and oxyferryl heme decay paralleled each other, with roughly comparable rates irrespective of peroxide structure. In contrast, the oxyferryl heme species was significantly less persistent than the tyrosyl radical in reactions with lower 15-HPETE levels. This uncoupling of the two redox centers has not been reported before for PGHS-1, although it has been noted for PGHS-2 (12). PGHS-1 contains “endogenous reductants” that are capable of peroxidase cycling (21, 23). With lower 15-HPETE levels, these internal cofactors may selectively deplete the oxyferryl heme, uncoupling its decay from that of tyrosyl radical. Our measurements using EtOOH/hydroquinone titrations suggest that the present batches of PGHS-1 contain 8–9 equiv of endogenous reductant. Evidence for peroxidase catalysis independent of events at the cyclooxygenase site has been reported (27), and such independence is recognized in recent mechanistic schemes (28). The divergence between oxyferryl heme and tyrosyl radical kinetics becomes more obvious at peroxide/heme ratios of >5 (Figure 6–Figure 8). This observation of divergence is strong evidence for the potential for independent reactions by the two oxidant species present in Intermediate II. It is expected that bifurcation of the decay kinetics of these two strong oxidant species is affected by the efficiency and level of both peroxide and cosubstrate.

Formation and Decay of Tyr385 Radical and Mn^{4+}=O during the Reaction of 15-HPETE with Mn-PGHS-1

The formation rate of Intermediate II in Mn-PGHS-1 during the reaction with 15-HPETE was approximately an order of magnitude slower than that of Fe-PGHS-1, consistent with previous observations (17). This is presumably due to slower Intermediate I formation (15–17) and fits well with the long lag phase observed for cyclooxygenase catalysis by Mn-PGHS-1 (30). Although the MnPPIX redox changes appeared to be somewhat faster than formation of tyrosyl radical with both 2 and 5 equiv of 15-HPETE, the difference may be due to the wavelength used for our kinetic measurement, 420 nm, which tracks not only the conversion from Intermediate I to Intermediate II but also the preceding step of Intermediate I formation, which is quite rapid (11). As our earlier data indicate that the Intermediate I [Mn(V)] species has a higher molar absorptivity than Intermediate II [Mn-(IV)], even low concentrations of Intermediate I may contribute significantly (11). Nevertheless, as in the case of Fe-PGHS-1, the formation of radical in Mn-PGHS-1 paralleled the formation of Mn(IV)=O reasonably well. This indicates that this portion of the catalytic mechanism of Mn-PGHS-1 is similar to that of Fe-PGHS-1 and suggests that substitution of the heme with MnPPIX does not disrupt the redox linkage between the metalloporphyrin and the tyrosyl radical.

When reacted with peroxide, Fe-PGHS-1 and Fe-PGHS-2 first form WD tyrosyl radical species and later WS species that are the sum of WD and NS components (2,25,26). For Fe-PGHS-2, the rapidly generated NS component originates from a second radical, on Tyr504 (31); the origin of the early NS in PGHS-1 is discussed below. For Mn-PGHS-1, there is only one WS tyrosyl radical whose line shape is distinct from those seen with Fe-PGHS-1 or -2 and does not change markedly as the reaction progresses from 4 ms to 10 s (Figure 4). If the Mn-PGHS-1 WS is comprised of WD and NS components, the equilibration between them must be rapid.

Oxyferryl Heme and Not Tyrosyl Radical Is Likely To Be Responsible for Peroxide-Induced Peroxidase Inactivation

To determine which oxidized species is responsible for peroxidase inactivation, the kinetics of inactivation were compared with the decay kinetics of oxyferryl heme and tyrosyl radical, the hypothesis being that decay of the oxidant involved should coincide with the decay of peroxidase activity. To ensure that substantial inactivation occurred, we used 20 equiv of peroxide without addition of exogenous cosubstrate, conditions that lead to a marked loss of peroxidase activity and heme Soret absorbance (23). For Fe-PGHS-1 reacted with excess EtOOH or 15-HPETE, the kinetics of peroxidase inactivation most closely correlated with loss of the oxyferryl heme absorbance, whereas the overall tyrosyl radical intensity remained largely unchanged during the period of inactivation (Figure 6 and Figure 7). There is no additional radical decay phase missing in the rapid-freeze quench dead time (4–5 ms) because we caught the radical formation phase in the reaction with EtOOH (Figure 6) and the same maximal extent, 0.5–0.6 spin/heme, of radical formation was also observed when 15-HPETE was used as the substrate (Figure 7). Further resolution of the tyrosyl radical EPR signal into the WD and NS components seemed to create a correlation between the WD decay and the peroxidase self-inactivation (0.19 s^{-1} vs 0.14 s^{-1} in Figure 6) in the EtOOH reaction. The NS EPR signal, originally assigned to an inactivation marker in PGHS-1 (23,32), was demonstrated to be a consequence of radical migration from Tyr385 to Tyr504 in both PGHS-2 (31) and PGHS-1 (C. Rogge et al., unpublished results). Such a radical migration process could not be the cause for peroxidase activity loss, as the total amount of tyrosyl radical essentially remained constant while the majority of the peroxidase activity was lost (Figure 6 and Figure 7). On the other hand, decoupling of oxyferryl heme and tyrosyl radical via radical migration may provide a pathway for cyclooxygenase inactivation which is independent of peroxidase inactivation. Such a hypothesis needs to be tested.

As a check on the plausibility of peroxidase inactivation due to oxyferryl heme, the kinetic data for absorbance at 428 nm and surviving peroxidase activity were compared with predictions of a mechanistic model, as described in Experimental Procedures. This minimal model has Intermediate II as the branching point to irreversible self-inactivation and assumes that Intermediate II consists of two discrete, noninteracting redox species, oxyferryl heme (Compound II) and tyrosyl radical. Published rate constants were used for k_1, k_2, k_5, k_6, and the extinction coefficients of each enzyme. As shown in Figure 9, the model generated reasonable predictions of the changes in both A_{428} and residual peroxidase activity for reactions with either EtOOH (panel A) or 15-HPETE (panel B) under the reaction conditions used for the experiments in Figure 6 and Figure 7. The main differences in modeling reactions with EtOOH and 15-HPETE are the higher values of k_1 and k_2 for 15-HPETE, consistent with published results (11). Also, the k_5 value in the EtOOH simulation is only 23% of that of the 15-HPETE simulation, but both are within the experimental range (0.2–2.0 s^{-1}) for Intermediate III formation (9). Only slight adjustments in the molar absorbance coefficients of heme intermediates were needed to produce optimal fitting for each peroxide substrate, indicating that the optical properties of enzyme intermediates are largely independent of substrate structure. Although the rate constants of the recycling steps of the high oxidation state intermediates by endogenous reductant, k_3 and k_4, were not measured, these values are all in the range (10^4–10^5 M^{-1} s^{-1}) observed for exogenous cosubstrates (3,33). A “residual” component was introduced to reflect the observation that the peroxidase activity never reached zero with either 15-HPETE (5% residual activity) or EtOOH (34% residual activity). Some of the persistent peroxidase activity may be due to nonenzymatic activity caused by free heme (34). The ability of the minimal model to reasonably fit reactions with both EtOOH and 15-HPETE is consistent with the participation of oxyferryl heme in peroxidase self-inactivation.

There are two distinct NS EPR species in PGHS-1; one of these is attributed to self-inactivated enzyme, and the other is observed with Fe-PGHS-1 complexed with cyclooxygenase inhibitors (2,26). It has been proposed that in the self-inactivated NS the radical continues to reside on Tyr385, while in the inhibitor-bound NS, the radical migrates to a different tyrosine residue (6). In PGHS-2, Tyr504 was identified as an alternative tyrosyl radical site both with and without the cyclooxygenase inhibitor (31). It seemed possible that destructive side reactions might be faster from tyrosyl radical at an alternative site, so the peroxidase inactivation of indomethacin-treated Fe-PGHS-1 was compared with that of the uninhibited enzyme. A NS EPR spectrum was seen at the earliest reaction time point in the reaction of indo-Fe-PGHS-1 with peroxide, yet peroxidase inactivation proceeded at the same rate as with untreated enzyme and the NS radical did not decrease in concentration or alter line shape with a rate correlated to the peroxidase activity decay (Figure 7 and Figure 8). This is an additional indication that tyrosyl radicals are not responsible for peroxidase inactivation.

Previous studies have shown that heme loses its native coordination during the inactivation process but is not chemically modified or covalently bound to the PGHS-1 protein (9). However, addition of fresh heme to inactivated PGHS-1 does not restore lost activity, indicating that the protein itself is modified in some way during inactivation (9). Given the current results that implicate the oxyferryl heme of Intermediate II in inactivation, oxidative damage of the side chains of functionally important amino acids in the heme vicinity may be the basis for loss of catalytic activity.

CONCLUSIONS

Intermediate II is a double-edged sword, being necessary for cyclooxygenase catalysis but also leading to self-inactivation. Once Intermediate II forms, its two strong oxidants can undergo further reactions independently. One of these oxidants, the Tyr385 radical, abstracts a hydrogen atom from AA to initiate cyclooxygenase catalysis, while the other oxidant in Intermediate II, oxyferryl heme, is linked to self-destructive side reactions. These two processes appear to control the catalytic activity of Fe-PGHS-1 during prostanoid synthesis. Both the peroxide level and the cosubstrate concentration and efficiency could control the extent of kinetic independence of the oxyferryl heme and tyrosyl radical in Intermediate II.

Acknowledgments

We thank Dr. Bijan Bambai for assistance with the Mn-PGHS-1/EtOOH RFQ experiments.

REFERENCES

1. Rouzer CA, Marnett LJ. Mechanism of free radical oxygenation of polyunsaturated fatty acids by cyclooxygenases. Chem. Rev 2003;103:2239–2304. [PubMed: 12797830]
2. Tsai A-L, Kulmacz RJ. Tyrosyl radicals in prostaglandin H synthase-1 and -2. Prostaglandins Leukotrienes Med 2000;62:231–254.
3. Lambeir AM, Markey CM, Dunford HB, Marnett LJ. Spectral properties of the higher oxidation states of prostaglandin H synthase. J. Biol. Chem 1985;260:14894–14896. [PubMed: 3934150]
4. Dietz R, Nastainczyk W, Ruf HH. Higher oxidation states of prostaglandin H synthase. Rapid electronic spectroscopy detected two spectral intermediates during the peroxidase reaction with prostaglandin G2. Eur. J. Biochem 1988;171:321–328. [PubMed: 3123232]
5. Shimokawa T, Kulmacz RJ, DeWitt DL, Smith WL. Tyrosine 385 of prostaglandin endoperoxide synthase is required for cyclooxygenase catalysis. J. Biol. Chem 1990;265:20073–20076. [PubMed: 2122967]
6. Tsai A-L, Hsi LC, Kulmacz RJ, Palmer G, Smith WL. Characterization of the tyrosyl radicals in ovine prostaglandin H synthase-1 by isotope replacement and site-directed mutagenesis. J. Biol. Chem 1994;269:5085–5091. [PubMed: 8106487]

7. Markey CM, Alward A, Weller PE, Marnett LJ. Quantitative studies of hydroperoxide reduction by prostaglandin-H synthase: Reducing substrate-specificity and the relationship of peroxidase to cyclooxygenase activities. J. Biol. Chem 1987;262:6266–6279. [PubMed: 3106353]
8. Marshall PJ, Kulmacz RJ, Lands WEM. Constraints on prostaglandin biosynthesis in tissues. J. Biol. Chem 1987;262:3510–3517. [PubMed: 3102488]
9. Wu G, Wei C, Kulmacz RJ, Osawa Y, Tsai A-L. A mechanistic study of self-inactivation of the peroxidase activity in prostaglandin H synthase-1. J. Biol. Chem 1999;274:9231–9237. [PubMed: 10092596]
10. Wu G, Kulmacz RJ, Tsai AL. Cyclooxygenase inactivation kinetics during reaction of prostaglandin H synthase-1 with peroxide. Biochemistry 2003;42:13772–13777. [PubMed: 14622024]
11. Tsai A-L, Wei C, Baek HK, Kulmacz RJ, Van Wart HE. Comparison of peroxidase reaction mechanisms of prostaglandin H synthase-1 containing heme and mangano protoporphyrin IX. J. Biol. Chem 1997;272:8885–8894. [PubMed: 9083007]
12. Tsai A-L, Wu G, Palmer G, Bambai B, Koehn JA, Marshall PJ, Kulmacz RJ. Rapid kinetics of tyrosyl radical formation and heme redox state changes in prostaglandin H synthase-1 and -2. J. Biol. Chem 1999;274:21695–21700. [PubMed: 10419480]
13. Hecker M, Ullrich V, Fischer C, Meese CO. Identification of novel arachidonic acid metabolites formed by prostaglandin H synthase. Eur. J. Biochem 1987;169:113–123. [PubMed: 3119336]
14. Kulmacz RJ, Lands WE. Requirements for hydroperoxide by the cyclooxygenase and peroxidase activities of prostaglandin H synthase. Prostaglandins 1983;25:531–540. [PubMed: 6410459]
15. Odenwaller R, Maddipati KR, Marnett LJ. Detection of a higher oxidation state of manganese-prostaglandin endoperoxide synthase. J. Biol. Chem 1992;267:13863–13869. [PubMed: 1321128]
16. Strieder S, Schaible K, Scherer HJ, Dietz R, Ruf HH. Prostaglandin endoperoxide synthase substituted with manganese protoporphyrin IX. Formation of a higher oxidation state and its relation to cyclooxygenase reaction. J. Biol. Chem 1992;267:13870–13878. [PubMed: 1629186]
17. Kulmacz RJ, Palmer G, Wei C, Tsai A-L. Reaction and free radical kinetics of prostaglandin H synthase with manganese protoporphyrin IX as the prosthetic group. Biochemistry 1994;33:5428–5439. [PubMed: 8180166]
18. Mizuno K, Yamamoto S, Lands WE. Effects of non-steroidal anti-inflammatory drugs on fatty acid cyclooxygenase and prostaglandin hydroperoxidase activities. Prostaglandins 1982;23:743–757. [PubMed: 6812164]
19. Graff G, Anderson LA, Jaques LW. Preparation and purification of soybean lipoxygenase-derived unsaturated hydroperoxy and hydroxy fatty acids and determination of molar absorptivities of hydroxy fatty acids. Anal. Biochem 1990;188:38–47. [PubMed: 2121063]
20. Kulmacz, RJ.; Lands, W. Prostaglandins and Related Substances: A Practical Approach. Benedetto, C.; McDonald-Gibson, RG.; Nigam, S.; Slater, TF., editors. Washington, DC: IRL Press; 1987. p. 209-227.
21. Tsai A-L, Wu G, Kulmacz RJ. Stoichiometry of the interaction of prostaglandin H synthase with substrates. Biochemistry 1997;36:13085–13094. [PubMed: 9335571]
22. Tsai A-L, Berka V, Kulmacz RJ, Wu G, Palmer G. An improved sample packing device for rapid freeze-trap electron paramagnetic resonance spectroscopy kinetic measurements. Anal. Biochem 1998;264:165–171. [PubMed: 9866678]
23. Tsai A-L, Palmer G, Kulmacz RJ. Prostaglandin H synthase. Kinetics of tyrosyl radical formation and of cyclooxygenase catalysis. J. Biol. Chem 1992;267:17753–17759. [PubMed: 1325448]
24. Wu G, Vuletich JL, Kulmacz RJ, Osawa Y, Tsai A-L. Peroxidase self-inactivation in prostaglandin H synthase-1 pretreated with cyclooxygenase inhibitors or substituted with mangano protoporphyrin IX. J. Biol. Chem 2001;276:19879–19888. [PubMed: 11279106]
25. DeGray JA, Lassmann G, Curtis JF, Kennedy TA, Marnett LJ, Eling TE, Mason RP. Spectral analysis of the protein-derived tyrosyl radicals from prostaglandin H synthase. J. Biol. Chem 1992;267:23583–23588. [PubMed: 1331091]
26. Shi W, Hoganson CW, Espe M, Bender CJ, Babcock GT, Palmer G, Kulmacz RJ, Tsai A-L. Electron paramagnetic resonance and electron nuclear double resonance spectroscopic identification and characterization of the tyrosyl radicals in prostaglandin H synthase-1. Biochemistry 2000;39:4112–4121. [PubMed: 10747802]

27. Koshkin V, Dunford HB. Coupling of the peroxidase and cyclooxygenase reactions of prostaglandin H synthase. Biochim. Biophys. Acta 1999;1430:341–348. [PubMed: 10082961]

28. Kulmacz RJ, van der Donk WA, Tsai A-L. Comparison of the properties of prostaglandin H synthase-1 and-2. Prog. Lipid Res 2003;42:377–404. [PubMed: 12814642]

29. Tsai A-L, Palmer G, Xiao G, Swinney DC, Kulmacz RJ. Structural characterization of arachidonyl radicals formed by prostaglandin H synthase-2 and prostaglandin H synthase-1 reconstituted with mangano protoporphyrin IX. J. Biol. Chem 1998;273:3888–3894. [PubMed: 9461572]

30. Hemler ME, Graff G, Lands WE. Accelerative autoactivation of prostaglandin biosynthesis by PGG2. Biochem. Biophys. Res. Commun 1978;85:1325–1331. [PubMed: 105736]

31. Rogge CE, Liu W, Wu G, Wang LH, Kulmacz RJ, Tsai AL. Identification of Tyr504 as an alternative tyrosyl radical site in human prostaglandin H synthase-2. Biochemistry 2004;43:1560–1568. [PubMed: 14769032]

32. Lassmann G, Odenwaller R, Curtis JF, DeGray JA, Mason RP, Marnett LJ, Eling TE. Electron spin resonance investigation of tyrosyl radicals of prostaglandin H synthase. Relation to enzyme catalysis. J. Biol. Chem 1991;266:20045–20055. [(1992) 267 (9), 6449 (erratum)]. [PubMed: 1657911]

33. Lambeir AM, Markey CM, Dunford HB, Marnett LJ. Spectral properties of the higher oxidation states of prostaglandin H synthase. Adv. Prostaglandin, Thromboxane, Leukotriene Res 1987;17A:25–28.

34. Dix TA, Marnett LJ. Conversion of linoleic acid hydroperoxide to hydroxy, keto, epoxyhydroxy, and trihydroxy fatty acids by hematin. J. Biol. Chem 1985;260:5351–5357. [PubMed: 3988758]

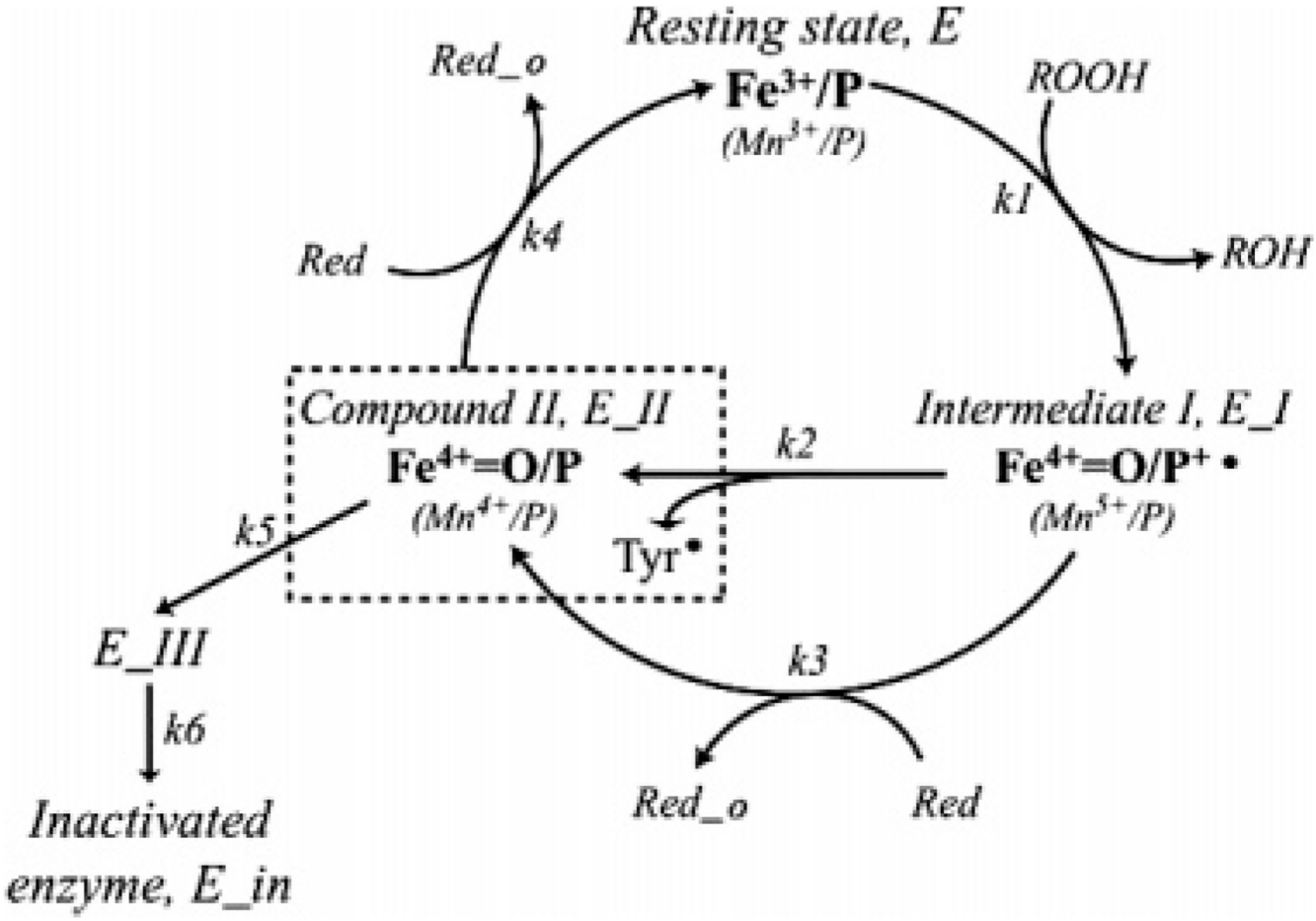

FIGURE 1.

Peroxidase mechanism of FePGHS-1 and MnPGHS-1 with hypothetical self-inactivation pathways, adapted from Dietz et al. (4) and Wu et al. (9). Fe^{4+}=O/$P^{+\bullet}$, oxyferryl heme with a porphyrin cation radical, or Mn^{5+} (Intermediate I); Fe^{4+}=O/P or Mn^{4+}=O/P, Compound II; Fe^{4+}=O/P or Mn^{4+}=O/P + $Tyr^{\bullet}$ (in dashed box), Intermediate II; ROOH, peroxide; ROH, alcohol; Red, reducing equivalent from cosubstrate; Red_o, reacted cosubstrate. Compound II and $Tyr^{\bullet}$ are shown as discrete oxidized components of Intermediate II to emphasize their redox independence. The oxyferryl heme of Compound II is proposed to lead to inactive forms of enzyme (E_III and E_in).

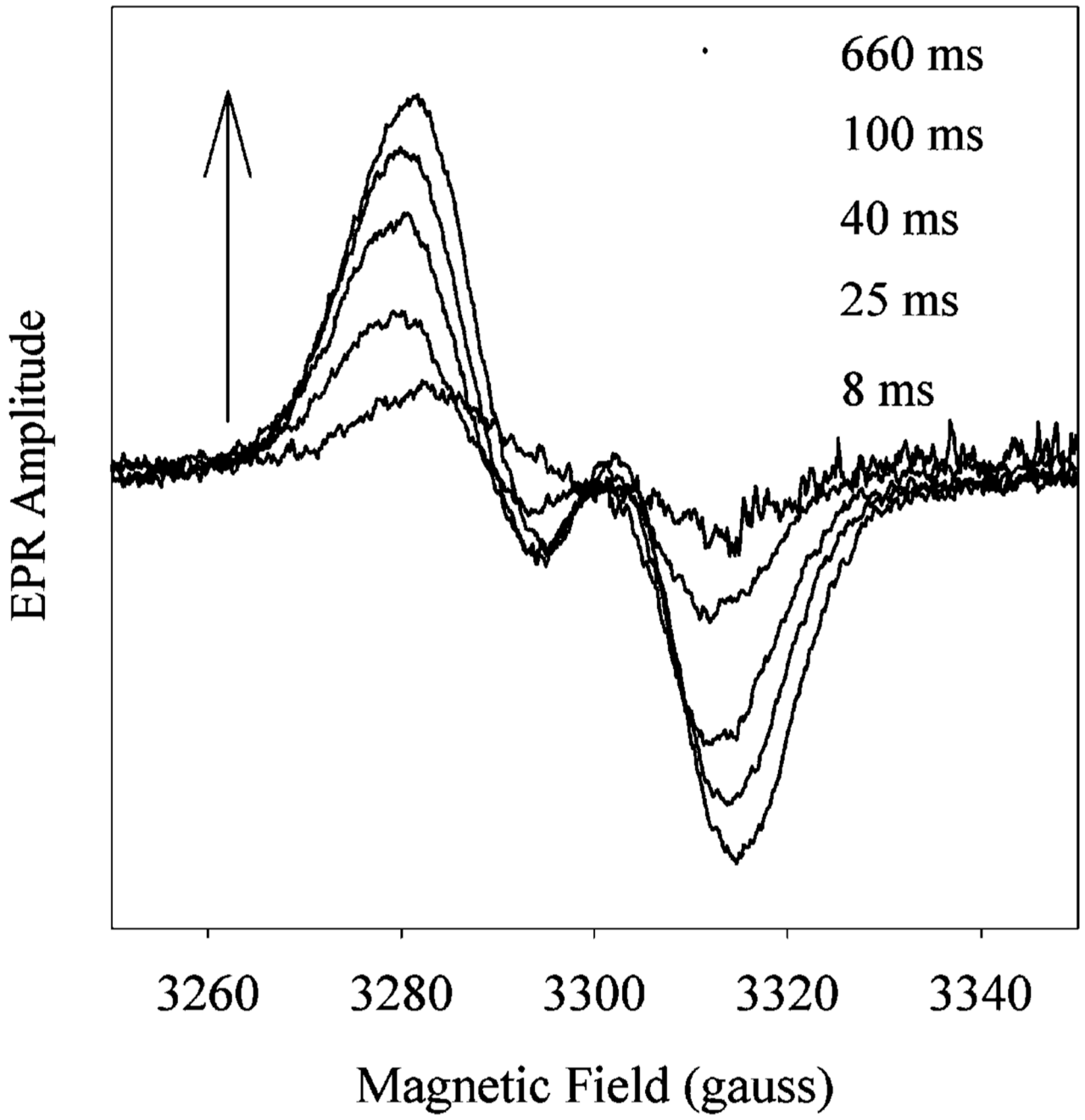

FIGURE 2.

EPR spectra of the tyrosyl radical formed during reaction of Fe-PGHS-1 with 15-HPETE. Fe-PGHS-1 samples (15 μM) in 100 mM KP_i (pH 7.2), 0.04% octyl glucoside, and 10% glycerol was reacted at room temperature with 5 equiv of 15-HPETE for the indicated times before freeze trapping. The arrow indicates the direction of intensity changes with time. EPR conditions: microwave power, 4 mW; frequency, 9.23 GHz; modulation amplitude, 3.2 G; temperature, 98 K.

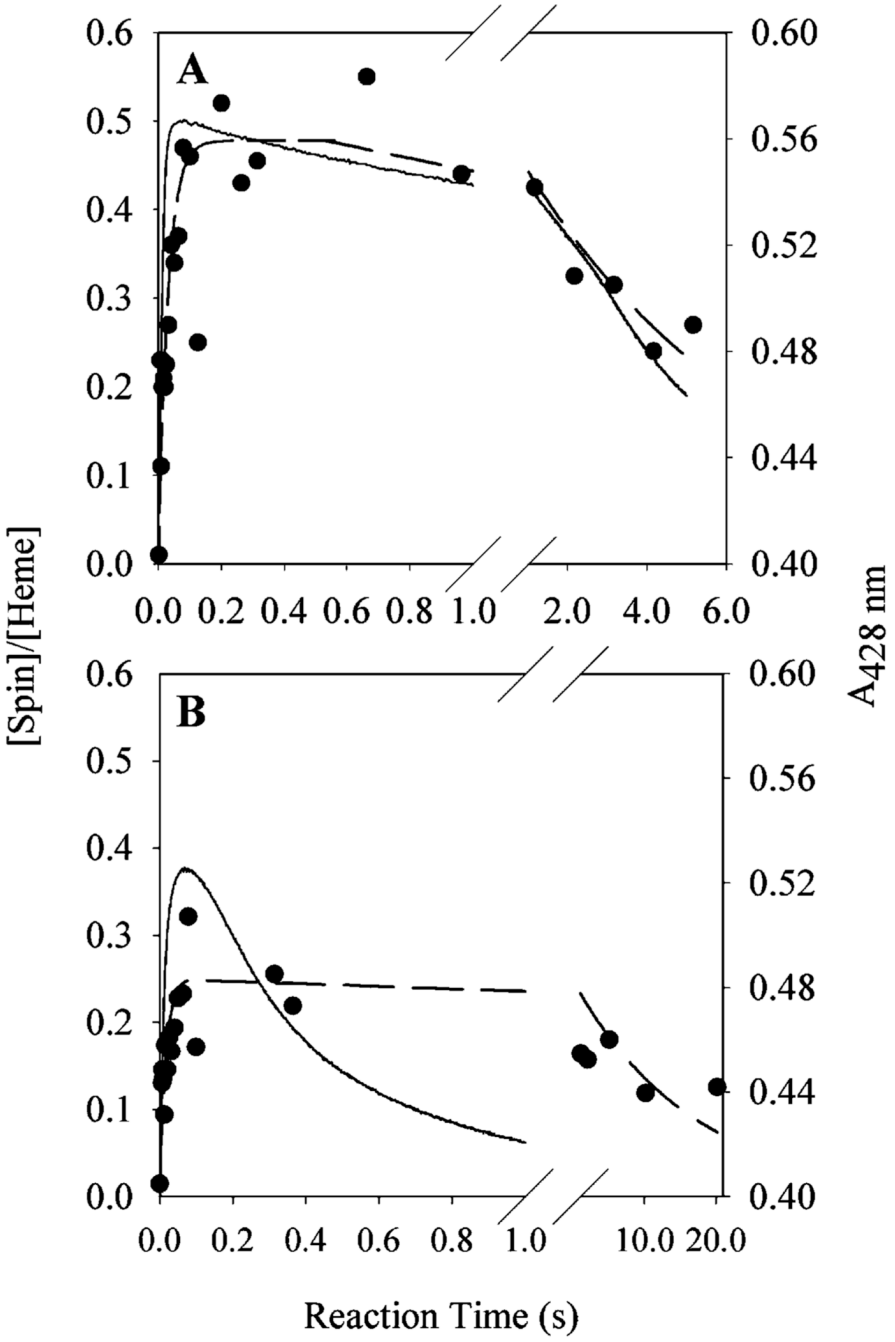

FIGURE 3.

Kinetics of tyrosyl radical and oxyferryl heme levels during reaction of Fe-PGHS-1 with 15-HPETE. Fe-PGHS-1 (15 μM) in 100 mM KP_i (pH 7.2), 0.04% octyl glucoside, and 10% glycerol was reacted at room temperature with either 5 (A) or 2 equiv (B) of 15-HPETE. Tyrosyl radical levels were determined by double integration of EPR signals such as those shown in Figure 2 (●), and oxyferryl heme levels were followed by A_{428} in parallel stopped-flow experiments (—). Dashed lines indicate exponential fits for tyrosyl radical formation and decay phases.

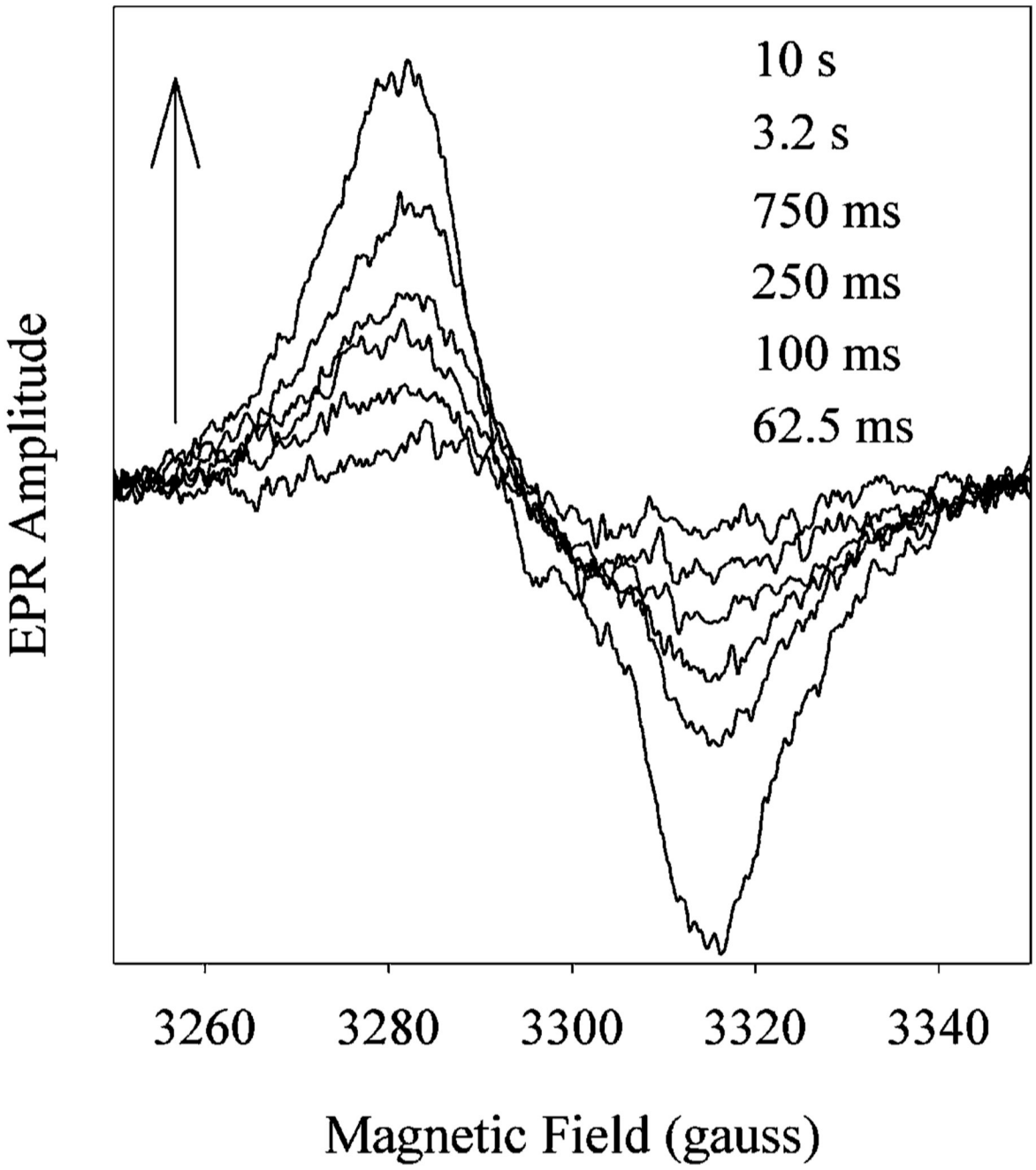

FIGURE 4.

EPR spectra of the tyrosyl radical formed during reaction of Mn-PGHS-1 with 15-HPETE. Mn-PGHS-1 samples (40 μM) in 100 mM KP_i (pH 7.2), 0.04% octyl glucoside, and 10% glycerol were reacted at room temperature with 2 equiv of 15-HPETE for the indicated times before freeze trapping. The arrow indicates the direction of intensity changes with time. EPR conditions are the same as those described in the legend of Figure 2.

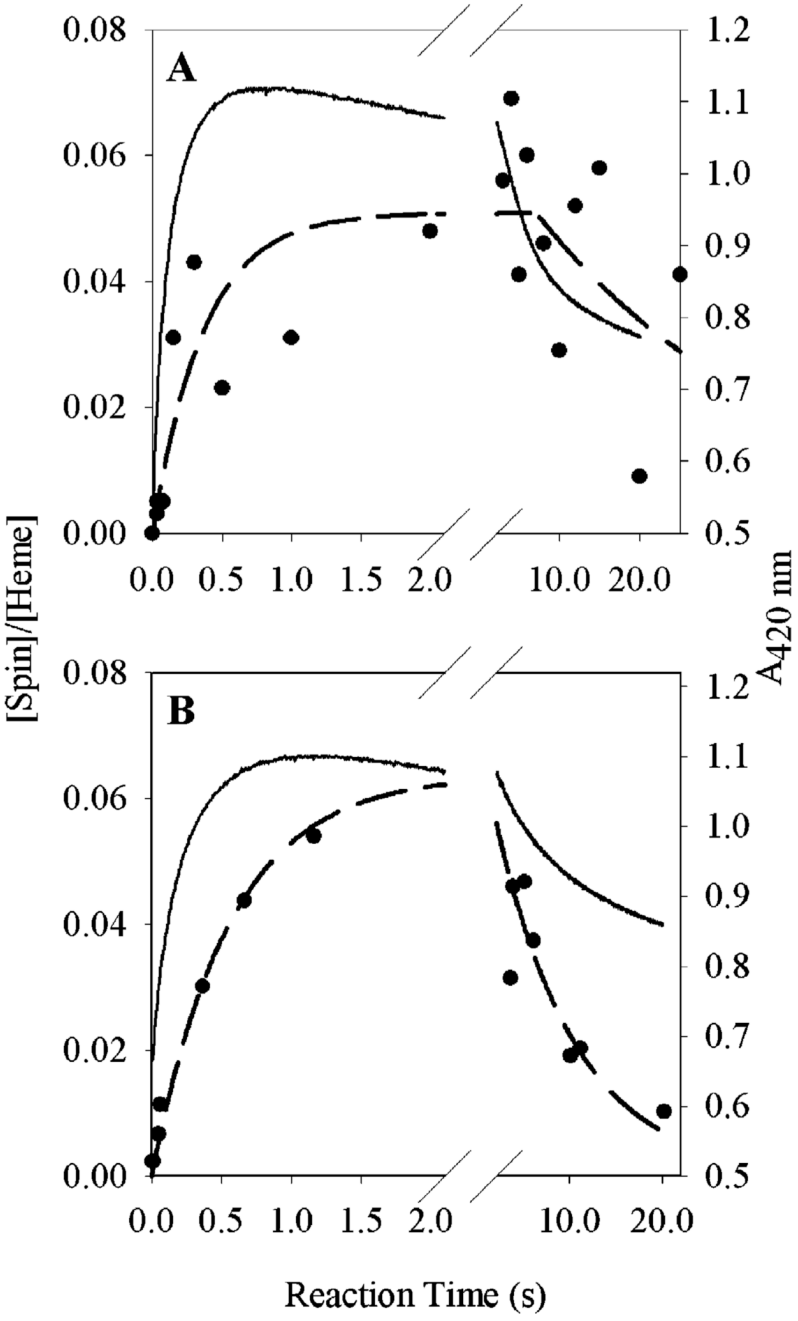

FIGURE 5.

Kinetics of tyrosyl radical and Mn^{5+}=O levels during reaction of Mn-PGHS-1 with 15-HPETE. Mn-PGHS-1 [(A) 18.5 and (B) 20 μM] in 100 mM KP_i (pH 7.2), 0.04% octyl glucoside, and 10% glycerol was reacted at room temperature with either 5 (A) or 2 equiv (B) of 15-HPETE. Tyrosyl radical levels were determined by double integration of EPR signals such as those shown in Figure 3 (●); Mn^{5+}=O concentrations are reflected by A_{420} in parallel stopped-flow experiments (—). Dashed lines indicate exponential fits for tyrosyl radical formation and decay phases.

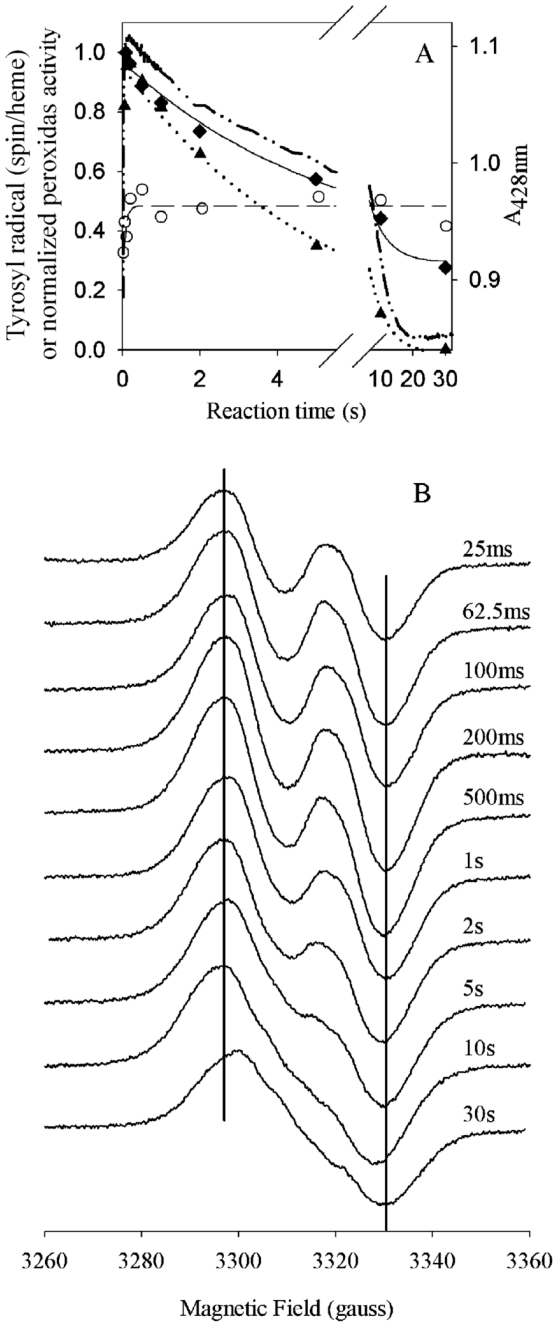

FIGURE 6.

Comparison of tyrosyl radical, oxyferryl heme, and peroxidase inactivation kinetics of Fe-PGHS-1 during reaction with EtOOH. Fe-PGHS-1 (30 μM) in 100 mM KP_i (pH 7.2), 0.04% octyl glucoside, and 10% glycerol was reacted with 20 equiv of EtOOH at room temperature. (A) Time courses of residual peroxidase activity (♦; fit,—), overall tyrosyl radical intensity (○; fit, — — —), deconvoluted WD tyrosyl radical intensity (▲; fit, •••), and oxyferryl heme (—••—). (B) EPR spectra from reaction samples freeze-trapped at the indicated times. EPR conditions: microwave power, 1 mW; frequency, 9.297 GHz; modulation amplitude, 2 G; and temperature, 114 K.

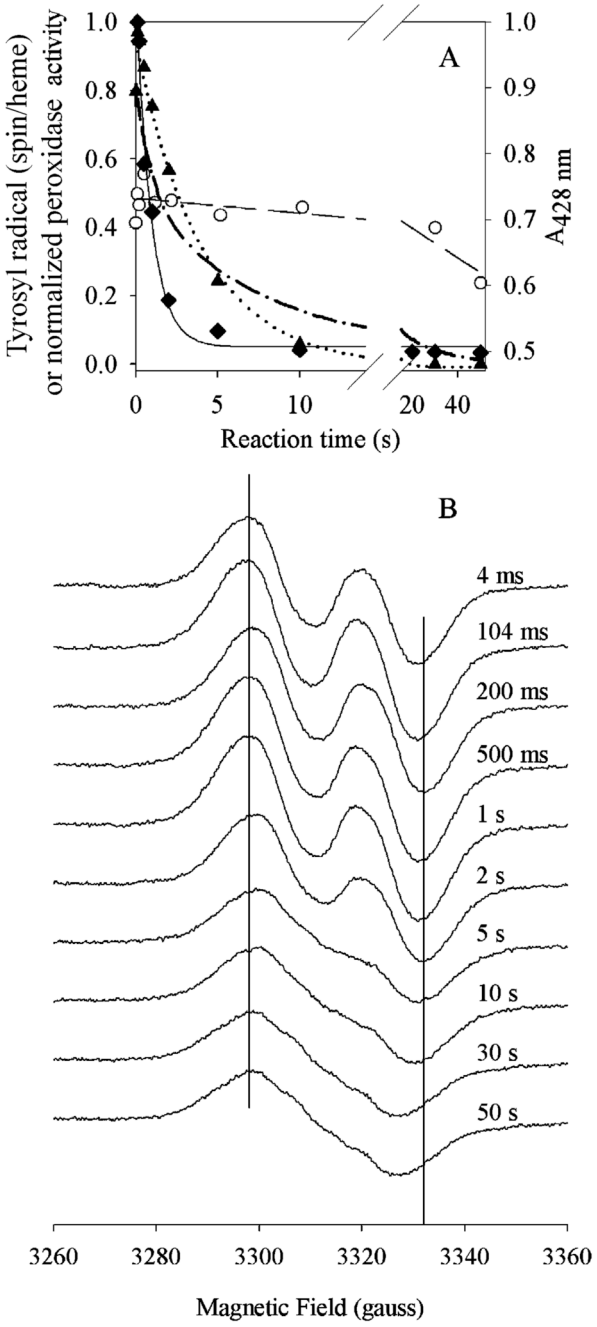

FIGURE 7.

Comparison of tyrosyl radical, oxyferryl heme, and peroxidase inactivation kinetics of Fe-PGHS-1 during reaction with 15-HPETE. Fe-PGHS-1 (30 μM) in 100 mM KP_i (pH 7.2), 0.04% octyl glucoside, and 10% glycerol was reacted with 20 equiv of 15-HPETE at room temperature. (A) Time course of residual peroxidase activity (♦; fit, ─), tyrosyl radical intensity (○; fit, ─ ─ ─), deconvoluted WD concentration (▲; fit, •••), and oxyferryl heme (─•─). (B) EPR spectra from reaction samples freeze-trapped at the indicated times. EPR conditions were the same as those described in the legend of Figure 6.

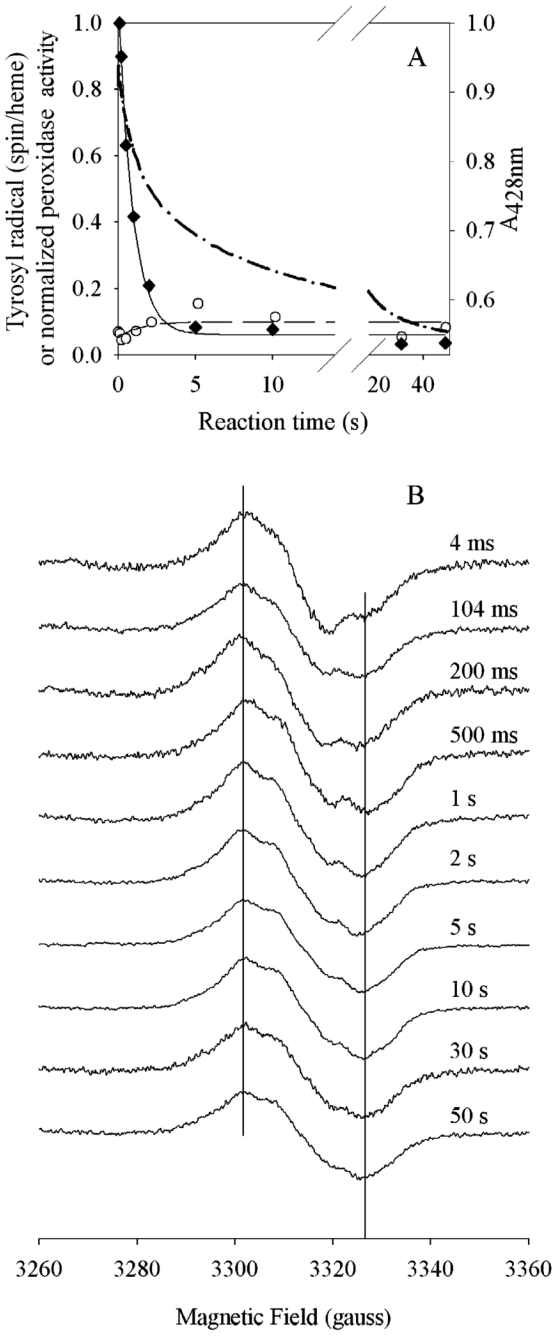

FIGURE 8.

Comparison of tyrosyl radical, oxyferryl heme, and peroxidase inactivation kinetics of indomethacin-treated Fe-PGHS-1 during reaction with 15-HPETE. Indo-Fe-PGHS-1 (30 μM) in 100 mM KP_i (pH 7.2), 0.04% octyl glucoside, and 10% glycerol was reacted with 20 equiv of 15-HPETE at room temperature. (A) Time course of residual peroxidase activity (♦; fit, ─), tyrosyl radical intensity (○; fit, ─ ─ ─), and oxyferryl heme (─•─). (B) EPR spectra from reaction samples freeze-trapped at the indicated times. EPR conditions were the same as those described in the legend of Figure 6.

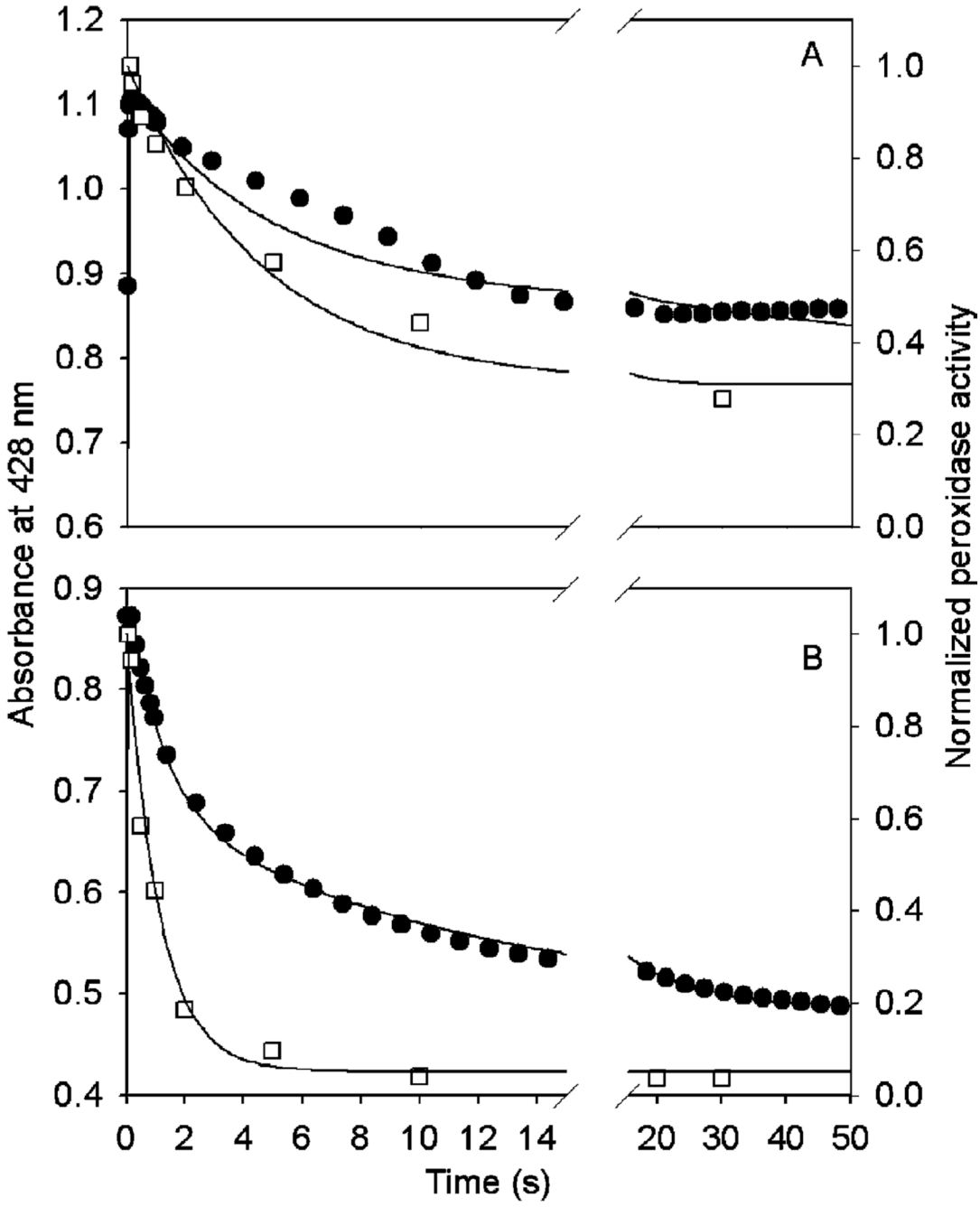

FIGURE 9.

Comparison of observed kinetics of A_{428} (●) and normalized remaining peroxidase activity (□) during reaction of Fe-PGHS-1 with 20 equiv of EtOOH (A) or 15-HPETE (B) from the experiments in Figure 6 and Figure 7 with computer simulations (—) generated as described in Experimental Procedures. The optimal values of rate constants for reaction with EtOOH are listed in Table 1, and the following parameters were used: ε1 = 0.063 μM^{-1} cm^{-1}, ε2 = 0.102 μM^{-1} cm^{-1}, ε3 = 0.080 μM^{-1} cm^{-1}, ε4 = 0.061 μM^{-1} cm^{-1}, and Residual = 0.34. The optimal values of rate constants for reaction with 15-HPETE are listed in Table 1, and the following parameters were used: ε1 = 0.060 μM^{-1} cm^{-1}, ε2 = 0.091 μM^{-1} cm^{-1}, ε3 = 0.068 μM^{-1} cm^{-1}, ε4 = 0.049 μM^{-1} cm^{-1}, and Residual = 0.05.

Table 1

Equations and Rate Constants Used for Kinetic Fitting

	rate constant	
equations for chemical reaction	**EtOOH**	**15-HPETE**
peroxidase reactions		
E + ROOH → E_I + ROH (a)	$k_1 = 1.0 \times 10^7\ M^{-1}\ s^{-1}$	$k_1 = 1.0 \times 10^8 M^{-1}\ s^{-1}$
E_I → E_II + Tyr• (b)	$k_2 = 80\ s^{-1}$	$k_2 = 320\ s^{-1}$
E_I + Red → E_II + Red_o (c)	$k_3 = 7.7 \times 10^4\ M^{-1}\ s^{-1}$	$k_3 = 1.0 \times 10^5\ M^{-1}\ s^{-1}$
E_II + Red → E + Red_o (d)	$k_4 = 1.0 \times 10^4\ M^{-1}\ s^{-1}$	$k_4 = 1.0 \times 10^4\ M^{-1}\ s^{-1}$
E_II → E_III (e)	$k_5 = 0.22\ s^{-1}$	$k_5 = 0.94\ s^{-1}$
E_III → E_in (f)	$k_6 = 0.005\ s^{-1}$	$k_6 = 0.092\ s^{-1}$
mass balance equations		
Total_E = E + E_I + E_II + E_III + E_in (g)		
ROOH = $Peroxide_{total}$ − ROH (h)		
Red = Reductant − Red_o (i)		
Active = (E + E_I + E_II)/Total_E + Residual(E_III + E_in)/ Total_E (j)		
A_{428} = ε1(E + E_I) + ε2(E_II) + ε3(E_III) + ε4(E_in) (k)		